

## Performance of an Active Stimulating Device Using a Rope Kite or Array in the Cod End to Reduce Juvenile by-catch

Yong-Hae Kim\*

*Institute of Marine Industry, Department of Marine Production technology, College of Marine Science, Gyeongsang National University, Tongyoung 650-160, Korea*

An active stimulating device (ASD) using a rope apparatus may operated by the flow of turbulence inside a cod end, generating variable stimuli in addition to flow-related effects to minimize the by-catch of juvenile fishes. Preliminary testing involved a hydrodynamic effect inside the cod end with a rotating rope kite or conical rope array to generate variable stimuli (visual stimuli, water flow, or physical contact with fish) to change fish position. The experimental rope kite offered more choice in rotating period and range of sweeping action; adjusting the towing line or flow velocity helped to drive fish toward the net panel and encouraged escape. The conical shape of the rope array in the cod end helped to clear a path for fish by disturbing the rigging and providing more contrast between objects, preventing an optomotor response. This enabled more black porgy to be herded toward the net at an early stage of towing. Therefore, either a conical rope array or a rotating rope kite can be used as an effective ASD to prevent juvenile by-catch.

Key words: Active stimulating cod end, Black porgy, Conical rope array, Rope kite

### Introduction

For decades, researchers worldwide have tried to minimize the by-catch of various juvenile fish, often by focusing on cod-end construction as a physical element that affects fish behavior in addition to biological factors (Wardle, 1993; Graham et al., 2004). Currently, most cod ends are designed to improve selectivity and thereby reduce by-catch using two main elements: square mesh windows and grid systems. The square mesh window used in some cod ends provides a clear path for juvenile fish to escape (O'Neill et al., 2006; Sala et al., 2008). It is now legally required in some countries to reduce the juvenile by-catch of most roundfish, but it is less effective for flatfish, which vary greatly by species. A grid system, combined with square mesh windows or guiding funnels, is widely used to reduce juvenile by-catch of prawn and shrimp and even other fish, but this kind of system has encountered problems related to its rigid construction (Cho et al., 2005; Grimaldo et al., 2008). Recent improvements have recently been made, such as the flexible grid (Angell and Lilleng, 2001; Massuti et al., 2009).

Glass and Wardle (1995) experimented with installing a 'black tunnel' canvas covering at the posterior of cod ends and were able to increase the escapement of juvenile fish by up to 70%. They explained that the black canvas resembled a predator to fish swimming in the forward section. However, this visual contrast requires maintaining relatively bright illumination and clear water, which are limited at certain fishing depths or under cloudy conditions. Other researchers have used guiding panels or funnel nets in addition to square mesh windows or grid systems in the cod end to separate or guide fish from nephrops (Polet et al., 2004; Bahamon et al., 2007; Ferro and Kynoch, 2007).

Despite the technological innovations described above, worldwide by-catch is estimated at about 20 million tons, although estimation is difficult for a variety of reasons (Chopin and Suuronen, 2009). Reducing by-catch using environmentally friendly commercial fishing methods will require broad management measures subject to international regulations. These management measures could include modifications to fishing gear, such as installation of by-catch reduction devices and other gear-based mitigation technologies, or use of alternative fishing gear and practices.

---

\*Corresponding author: yonghae@gnu.kr

Almost all by-catch reduction methods involve providing a clear visual path for juvenile fish; for example, square mesh windows in a trawl cod end have a wider mesh opening than diamond mesh windows (Wardle, 1993). The grid device attached in the middle section of a cod end usually has longer slits, increasing the possibility that smaller creatures (such as prawn or flatfish) can separate (Massuti et al., 2009). However, these methods are classified as passive stimuli for fish because nets and other devices maintain a constant position based on towing speed, so visual stimuli and flow schemes also remain constant. Macbeth et al. (2005) have criticized attempts to reduce by-catch by simply increasing mesh openings rather than including modifications to devices in the cod end.

O'Neill et al. (2003) observed and analyzed the pulsing motion of the cod end induced by vessel and wave motion to assess the relationship between the pulsing cod end and fish escapement during poor weather. The shaking action observed in the cod end can act as a sieve for fish, suggesting that turbulent flow or changes in visual stimuli may voluntarily or forcibly remove fish from the cod end. Fish escapement from the cod end was greater when mesh nets were used in North Sea trawls, where movement was very erratic and prevented fish from maintaining position as an optomotor response (Kim et al., 2008). In addition, Jones et al. (2008) found that rates of netting strikes of fish during North Sea trawling were generally higher at higher towing speeds and lower catch densities. They hypothesized that opportunistic contact occurred during netting, perhaps as a result of the pulsing motion of the cod end and water turbulence rather than any active change in behavior.

Based on these findings, it is feasible that active fluttering or shaking of a net could be used as an active stimulating device to encourage fish to approach the net and then easily escape from the cod end. In principle, active motion of a device in the cod end could first drive fish voluntarily to approach the netting (i.e., interfere with optomotor swimming response by changing visual stimuli); then, more turbulent shaking of the cod end could ensure that fish are passively moved away.

Studies have demonstrated that the cod end in a bottom trawl has a posterior circular expanding shape that increases in relation to the size of the catch, while the diameter decreases in the anterior of the cod end (Robertson, 1986; O'Neill et al., 2003). Changes in cod end shape appear to be gradual and somewhat catch dependent and to depend on towing time. In addition, a pulsing motion in the cod end to reduce

by-catch would be difficult to accomplish in generally calm weather. Additional active stimuli are therefore necessary, possibly using flexible materials such as fishing gear components, operating at high levels of performance during towing under any weather conditions or in an underwater environment.

Therefore, an active stimulating device (ASD) proposed such as additional rope rigging apparatus can change position relatively by a turbulent flow inside the cod end, resulting in variable stimuli (Kim and Wardle, 1998; Broadhurst et al., 1999). In this study, a kind of rope kite was developed, and its operating characteristics were measured as it rotated continuously in a circulating water tank. This rope kite with pendants exhibited good potential as it rotated and changed stimuli including visual stimuli, water flow, and physical contact with fish. In addition, a conical rope array was tested as a stimulating device; it was fixed inside a cod end, and the responses of black porgy were observed in field experiments. The results demonstrated that both the rotating rope kite and conical rope array exhibited high potential for practical use as active stimulating devices in the cod end of towed fishing gear.

## Materials and Methods

Two kinds of active stimulating devices were constructed for the model experiments: a rotating rope kite and a conical rope array installed inside the cod end. The rope kite was made from braided PA (Polyamide) rope ( $\varnothing$  12 mm, cord length of 20 cm), connecting bridles (braided PA twine,  $\varnothing$  3.5 mm, 5 and 10 cm respectively), and towing line (braided PA twine,  $\varnothing$  3.5 mm, 115 cm) with a swiveling end, as shown in Fig. 1. Two tail pendants (braided PA twine,  $\varnothing$  3.5 mm) were also attached, one at the leading edge and one at trailing edge of the rope kite, to allow a wider range of motion. The 20 cm cord length was determined based on the stiffness of the rope. This underwater rope kite has a lifting force with an adjustable angle of attack using the two bridle lengths; it can also rotate counterclockwise in response to the imbalance between the lifting force and the weight of the tail pendant, similar to the lateral circling motion of a kite in the air (Stevenson et al., 2005; Houska and Diehl, 2006; Sánchez, 2006). This imbalance, which works as a lifting force, results in differences between the leading edge and trailing edge of the rope kite and consequently in shearing force as the rope kite rotates (Diehl et al., 2004; Canale et al., 2010).

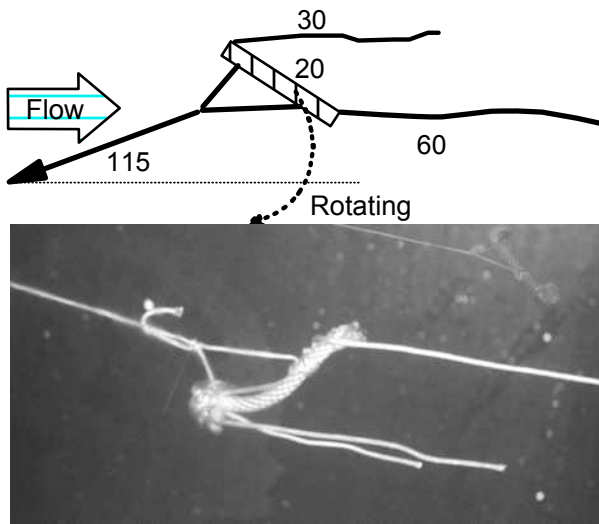


Fig. 1. Dimension of the rope kite as an active stimulating device (top, unit in cm) and the rope kite rotating action in the water tank (bottom, flow is to the right).

Testing first assessed whether the tail pendants caused good rotation of the rope kite. The frontal view was recorded using an underwater video camera (Huhu UVC-150) connected to a video recorder (Samsung SV-300WD), and the lateral view was recorded using a camcorder (LG GS-E600). Model experiments were carried out in a vertical circulating water channel located at Pukyong National University, which has the following parameters: size 6.0 [L] × 2.2 [B] × 1.4 [D] m and flow velocity ranging from 0.01 to 1.2 m/s (deviation  $\pm 0.4\%$  at 1.0 m/s). In this experiment, flow velocity was varied from 0.65 to 1.05 m/s, as measured by Marsh McBirney 201D.

In the water tank experiments, the position of the rope kite from a frontal view was defined in two dimensions (depth and transverse axis to flow), and relative coordinates were measured in millimeters to scale, with OHP films depicted at 0.2 s intervals on the LCD monitor (IMR, 15 in). Actual changes in kite position were estimated using a scale calibration derived from the video images.

The conical rope array consisted of white braided PA twine ( $\varnothing$  5 mm, length 1.2 m) in the model cod end (circular wire ring diameter 1 m, length 2.5 m) made of diamond knotless netting (PE  $\varnothing$  3.5 mm, mesh size 61 mm) with a hanging ratio of 80%, as shown in Fig. 2(A). Field towing experiments were carried out only for the conical rope array inside the cod end frame. Black porgy (*Acanthopagrus*

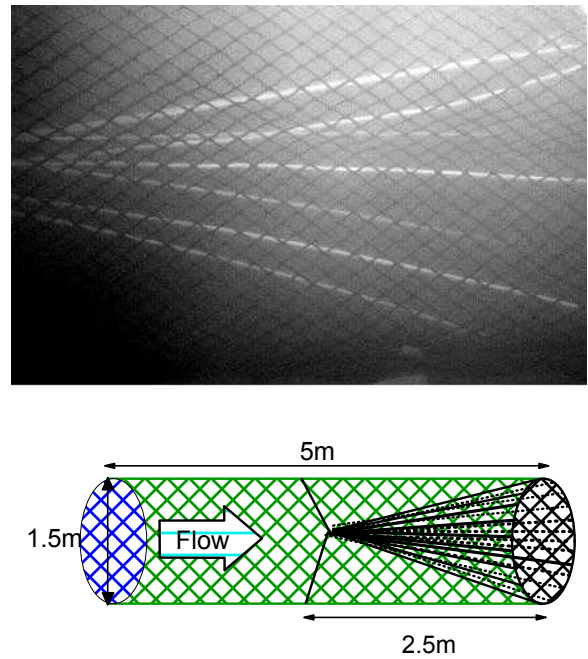


Fig. 2. The conical rope array inside cod-end (mesh size 61 mm) in the water tank experiments (top) and in field towing experiments (mesh size 120 mm) (bottom).

*schlegelii*) were caught using set nets off the Tongyoung coast in the early morning on 27 October 2005. One hundred fish were immediately transferred to three 450 liter plastic aerated tanks aboard the training ship SAEBADA. The fish were held in a resting state for at least 4 hours prior to experimentation. Following the towing experiments, each fish was measured for total length, weight, and girth.

Towing experiments were conducted at sea using a towing frame (5.0 [L] × 2.0 [B] × 1.5 [D] m, constructed from 10-mm-diameter stainless steel) with the cod end fitted according to the method described by Kim and Jang (2005). The experimental cod end was constructed from 120 mm diamond mesh using PE 120 ply twine, as shown in Fig. 2(B). The conical rope array was made from 23 sections of white braided PA rope ( $\varnothing$  12 mm, length 2.5 m) bound together at their anterior ends and fixed at the center line.

Towing trials were conducted in the Sea of Chudo, Tongyoung, Korea, during three tows using fresh groups of 30 fish per tow. Fish were moved from the plastic tanks to the cod end using a dip net and then towed at a speed of 1.1-1.6 m/s and a depth of 7-10 m, as measured by the SAEBADA's Simrad Trawl Eye System. Fish movement was monitored using two underwater video cameras (Simrad OE1324 and

Huhu UVC-150) mounted on the towing frame (see Kim and Jang, 2005) and recorded by two video recorders (Samsung SV-300WD and LG LV-R33). Each group of 30 fish was towed for approximately 30 min or until most of the fish were exhausted. Towing speed was measured using a Doppler log (Tokimec TD-310) aboard the training ship. During the sea experiments, seawater temperature was 20°C, and salinity was 33 psu, as measured by YSI85 (YSI, Inc.).

Changes in fish position during the field towing experiments were analyzed at 1 min intervals using a scale derived from visible mesh size. The shortest distance from a fish to the net was defined and estimated as the distance from the fish snout to the net panel of the cod end; these data were obtained using the rear view of the video images. In this experiment, herding response was defined as fish approaching within 30 cm of the net; the number of herding fish was counted at every minute for each group of 30 fish during each 30 min tow.

## Results and Discussion

The rope kite was a successful active stimulating device for fish, rotating counterclockwise along the center line of the towing point from the frontal view with rotating periods and amplitude by flow velocity under given specifications. The rotating periods and power index decreased with increasing flow velocity and were much longer with tail pendants (number of data  $n=49$ ) than without tail pendants ( $n=46$ ), as shown in Fig. 3. Therefore, the rotating period of a rope kite can be controlled by the length of the tail pendant and towing line, as well as the lifting force by the cord of the rope kite in relation to the angle of attack (Stevenson et al., 2005; Houska and Diehl, 2006; Sánchez, 2006).

Figs. 4 and 5 present examples of the rotating traces. Rotating amplitude is represented as a two-dimensional frontal view of depth and transverse direction to the flow for four points on the rope kite at a flow velocity of 0.7 m/s when the rotating period was 5.2 s, and at a flow velocity of 1.0 m/s when the rotating period was 4.4 s. The shape of the rotating trace was almost circular in most cases, although some irregularity in trace shape was observed, possibly due to imbalanced force or turbulent flow. When flow velocity was 0.7 m/s, the approximate diameter of the rope kite trace was about 40 cm at the kite leading edge, 30 cm at the kite trailing edge, 40 cm at the end of head pendant from the kite leading edge, and 30 cm at the end of the pendant from the

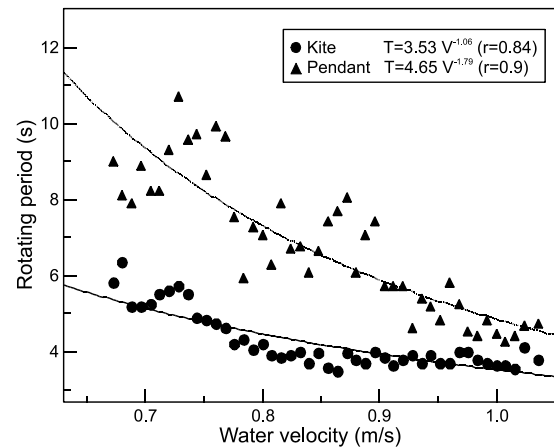


Fig. 3. The relationship between rotating period of the rope kite with or without tail pendants and flow velocity in water tank experiments.

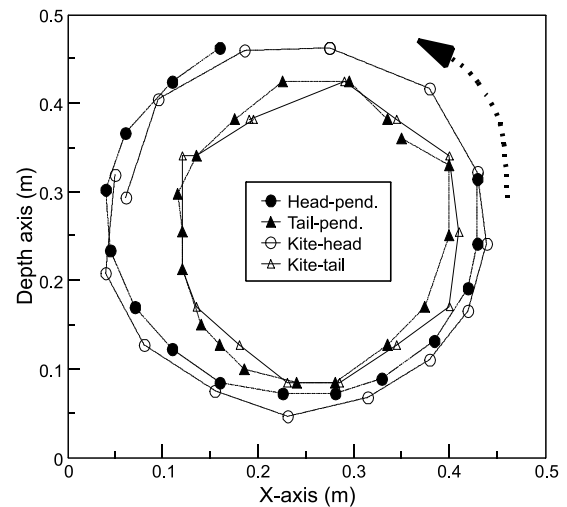


Fig. 4. The rotating traces from the frontal views in relation to parts of rope kite when flow velocity 0.7 m/s.

kite trailing edge. Thus, trace diameters of head parts were 10 cm longer than those of tail parts at flow velocities of 0.7 m/s and 1.0 m/s.

When flow velocity was 1.0 m/s, rotating traces of the rope kite had a diameter of approximately 30 cm at the leading edge of the kite, 25 cm at the trailing edge of the kite, 40 cm at the end of the head pendants, and 30 cm at the end of the tail pendants. Thus, trace diameters of head parts (kite leading edge and head pendant) were 10 cm longer than those of tail parts (trailing edge and tail pendant), and diameters at the ends of the pendants were 10 cm longer than the rope kite when flow velocity was 0.7 m/s.

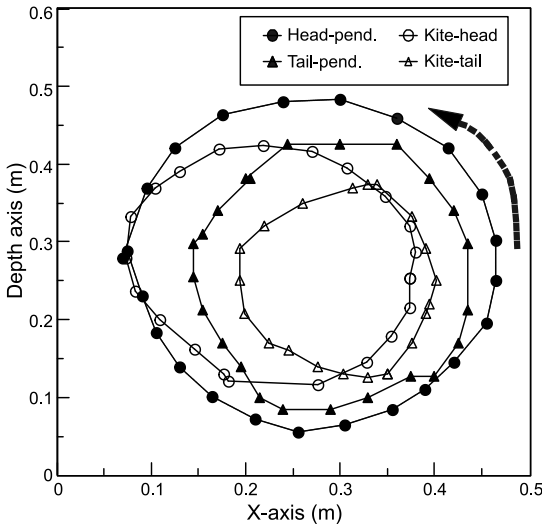


Fig. 5. The rotating traces from the frontal views in relation to parts of rope kite when flow velocity 1.0 m/s.

These 10 cm differences in trace diameter between head and tail parts at both water velocities can be estimated as the sine function of a 30° angle of attack of the rope kite by a 20 cm cord length as  $20\text{ cm} \times \sin 30^\circ = 10\text{ cm}$ . Rotating diameters at the two ends of the pendants were similar at both flow velocities (0.7 and 1.0 m/s), whereas the rotating diameter at the leading edge or trailing edge of the rope kite was 5-10 cm shorter when flow velocity was 1.0 m/s than when flow velocity was 0.7 m/s. These differences by flow velocity are probably related to rotating period and the resulting imbalance among lifting force, drag, and weight of tail pendants; more research is required to clarify these factors.

Diameter of the rope kite trace can be simply estimated as a two-dimensional equilibrium of the force acting on the rigid kite system at a given moment using a circular cylinder (Jackson, 2005; Williams et al., 2007; Vaikil and Green, 2009), as shown in Fig. 6.

Let towing line S be straight during rotation, as it was relatively short, with an angle  $\theta$  of towing line from the towing point. Tension T of the towing line at the towing point can be expressed as the vector of resultant lifting force L (as total lifting force L minus total weight W) and total drag D by towing line (abbreviation t), bridles (b), kite (k), and pendants (p) as follows:

$$D = T \cos \theta \quad L = T \sin \theta \quad (1)$$

$$\theta = \tan^{-1}(L/D) \quad (2)$$

$$D = Dt + Db + Dk + Dp \quad L = Lt + Lb + Lk + Lp - W \quad (3)$$

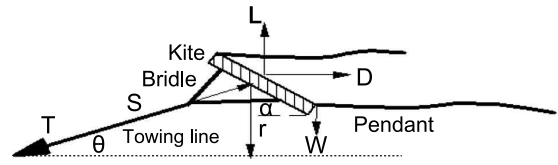


Fig. 6. The forces acting on the rope kite in 2-dimensional lateral plane for instant.

All parts of the rope kite were made of twine and can be considered a simplified circular cylinder with diameter  $d$  and length  $l$ . Then, drag or lift force under conditions of flow velocity  $V$  and water density  $\rho$  can be expressed with drag coefficient  $C_D$  and lift coefficient  $C_L$  as follows:

$$D = C_D / 2 \rho d l V^2 \quad L = C_L / 2 \rho d l V^2 \quad (4)$$

Coefficients  $C_D$  and  $C_L$  are functions of Reynolds number, angle of attack ( $\alpha$ ), aspect ratio ( $l/d$ ), surface roughness, fluctuation, etc., derived from the circular cylinder cases (Schlichting, 1979; Chakroun et al., 1996; Winkel and Paschen, 2005). To simplify the braided rope, coefficients were assumed to change linearly with the angle of attack as follows:

$$C_D = C_{D(\alpha=0)} + \beta \sin \alpha \quad (5)$$

$$C_L / C_D = C_{D/L(\alpha=0)} + \eta \sin 2\alpha \quad (6)$$

where  $\beta$  and  $\eta$  are slopes.

Based on previous data on drag and lift coefficients of a circular cylinder (Schlichting, 1979; Norberg, 2003; Winkel and Paschen, 2005; Gavaldà et al., 2009; Vaikil and Green, 2009), the coefficients for the braided PA ropes used in this experiment (diameter 3-12 mm) with surface roughness, an aspect ratio of 10, and a Reynolds number of  $1.5 \times 10^5$  were estimated at  $C_D = 0.1$  at  $\alpha = 0^\circ$ ,  $C_D = 1.0$  at  $\alpha = 90^\circ$ ,  $C_L / C_D = 0.05$  at  $\alpha = 0^\circ$ , and  $C_L / C_D = 0.5$  at  $\alpha = 45^\circ$ . Next, slopes for Eqs. 5 and 6 were derived as  $C_{D(\alpha=0)} = 0.1$ ,  $\beta = 0.9$ , and  $C_{D/L(\alpha=0)} = 0.05$ ,  $\eta = 0.45$  respectively. During rotation of the whole kite rigging, the rope kite itself had an outward lifting force, whereas the towline and bridles had an inward negative lifting force. By substituting relevant factors into Eqs. 6, 5, 4, and 3, the angle of towline  $\theta$  was estimated at 7-10° when  $V = 0.7-1.0$  m/s based on Eq. 2. The rotating radius  $r$  with  $S = 120$  cm was estimated using  $S \sin \theta$  as 15 cm when  $V = 0.7$  m/s and 21 cm when  $V = 1$  m/s; these results are very similar to the measurements obtained from the video images.

Based on the above results, the rotating rope kite used as an active stimulating device had varying

periods and range of action and should be considered for application in cod ends to reduce juvenile by-catch. The pulsing motion of the cod end affected the escape of juvenile haddock in the North Sea bottom trawl; the period of the cod end was 4-8 s due to trawler motion when wave heights were 1.7-2.8 m (O'Neill et al., 2003). Kim and Jang (2005) estimated the period of the swimming pattern of black porgy in the cod end to be about 3-5 s, and Kim and Wardle (2006) estimated the period for acceleration of the swimming speed of flatfish near a ground rope to range from 2 to 4 s. The rotating period of the rope kite in this experiment was similar to these results and might act to intervene or disturb steady swimming rhythms such as an optomotor response (Wardle, 1993; Kim and Wardle, 2008). The rotating range of the rope kite actually had a conical shape from the connecting point of the fore towing line to the end of kite pendants in three-dimensional space. The volume of the rotating rope kite with pendants could cover nearly half of the cod-end area, with the practical effect of disturbing fish swimming through visual and tactile stimuli and turbulent flow. This stimulating effect should disrupt fish response by varying the position of visual objects, as well as by driving fish to approach the net panel through tactile stimulus, enabling easy escape.

In general, when more fish approach netting, more are likely to escape from the cod end (Kim et al., 2008). Jones et al. (2008) observed that the fluttering of square mesh windows or slack nets in the cod end improved juvenile fish escape, although they did not provide any specific data about escape ratios, etc. The experimental rope kite used in the present study was more changeable in its rotating period and has a wider range of action, so it acted as a very active stimulating device to evoke fish escape response from the cod end. Further study will be necessary to investigate stimulating effects of the rope kite on fish escape from the cod end and its practical application to real fishing gear.

The conical rope array in the model cod end was observed to check the rigging and shape in the circulating water tank at a flow velocity 0.65-1.05 m/s. The rope rigging looked appropriate, and the shape of the conical rope array was steady, with a little flapping due to water flow, as shown in Fig. 2. Therefore, the conical rope array is expected to guide fish from the anterior binding point of the rope array in a narrow area to the side net panel in addition to providing visual contrast stimuli, although no wide motion occurred as with the rotating rope kite described above.

The towing experiment for the conical rope array in the cod end was carried out on black porgy as compressiform in the sea near Tongyoung. The 90 black porgy used in these towing experiments had a mean total body length of  $24.5 \pm 4.1$  cm, body girth of  $19.6 \pm 3.0$  cm, and body weight of  $284.6 \pm 111.6$  g. Body length distribution was nearly normal; Fig. 7 shows the cumulative frequency. Most of the fish used in these towing experiments had a smaller girth to the perimeter of 120 mm mesh, so they could pass easily through the cod-end mesh if they tried to escape.

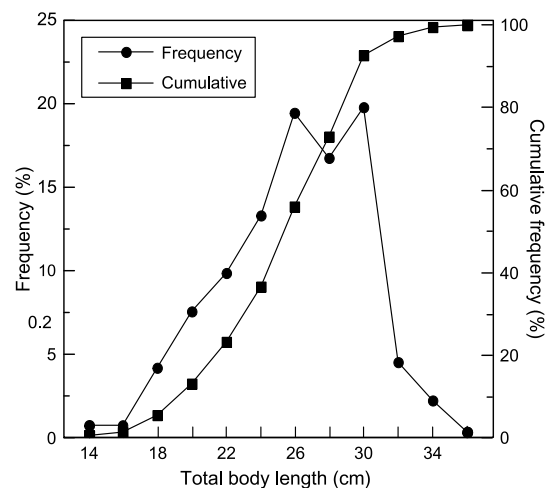


Fig. 7. Frequency distribution of total body length of black porgy used in towing experiments.

In the initial stages of the cod-end towing experiments, the fish were guided and herded from the central binding point of the conical rope array especially in the forward section (see Fig. 8), while in the rear section, they mainly exhibited an optomotor response. The herded fish approached the side net panel and frequently tried to pass through the mesh; some fish escaped successfully. With elapsed towing time, some fish swimming at the rear section of the cod end maintained stable swimming speed but then exhibited erratic or panicked responses such as sudden darting away and kicking forwards (Main and Sangster, 1991; Kim and Wardle, 2003; Kim et al., 2008). These erratic or panicked fish tended to move forward, but were disturbed by the conical rope array, which caused some fish to turn and swim back again, while others continued to move forward beside the rope array.

Herded fish were observed and counted within the ranges of the two cameras, which were positioned within 30 cm of the side net panel. Fig. 9 shows the

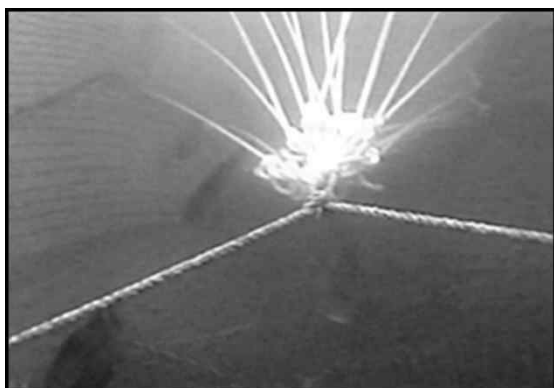


Fig. 8. Photo as a rear view shows fish swimming under the conical rope array in field towing experiments.

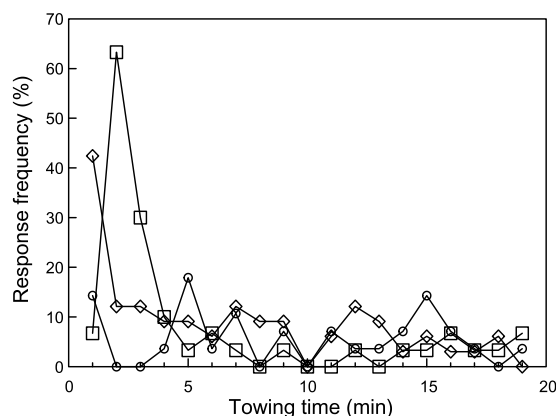


Fig. 9. Herding response frequency of a black porgy to approach to the side net panel of the cod-end beside the rope array in relation to the towing time elapsed.

herding ratio ( $N_H/30$ ) of the number of observed herded fish ( $N_H$ ) by each minute for each group of 30 black porgy. In two towing trials, the herding ratio generally decreased with elapsed towing time, possibly due to increasing numbers of escaping or exhausted fish. After three trials of 30 min towing had been completed, nearly half of the 90 fish remained in the cod end in an exhausted state. The shape and position of the rope array in the cod end affected the clear path of fish swimming by disturbing the optomotor response, which is main cause of fish remaining in the cod end until they are caught (Wardle, 1993; Kim et al., 2008). In addition, the rear view image of the diagonal rope array may appear to fish as a different contrast, which would remove the clear fixed object necessary for maintaining the optomotor response. Consequently, the conical rope array could help herd fish sideways,

resulting in a high probability of fish passing through the mesh. Further experiments will be necessary to compare herding and escape ratios with and without use of the conical rope array, and tests using more fish should be conducted to determine the effect and practicality of installing this system in the field.

## Acknowledgments

The author thanks Prof. C.W. Lee and M.Y. Choi for use of the circulating water tank at Pukyong National University, the crew of the Training Ship SAEBADA for help with the sea experiments. This work was supported by a Korea Research Foundation Grant funded by the Korean Government (MOEHRD) (KRF-2008-313-F00077).

## References

- Angell S and Lilleng D. 2001. New type of size selective system made of plastic and rubber: The "Flexgrid". 9<sup>th</sup> Joint Russian-Norwegian Symposium, "Technical regulations and by-catch criteria in the Barents Sea fisheries", PINRO Murmansk, Russia, 14-15 Aug. 2001. 108-112.
- Bahamon N, Sardà F and Suuronen P. 2007. Selectivity of flexible size-sorting grid in Mediterranean multi-species trawl fishery. *Fish Sci* 73, 1231-1240.
- Broadhurst MK, Kennelly SJ and Eayrs S. 1999. Flow-related effects in prawn-trawl codends: potential for increasing the escape of unwanted fish through square-mesh panels. *Fishery Bull* 97, 1-8.
- Canale M, Fagiano L and Milanese M. 2010. High altitude wind energy generation using controlled power kites. *IEEE Trans Cont Syst Technol* 18, 279-293.
- Chakroun WM, Abdel-Rahman AA and Taylor, R.P. 1996. Effect of surface roughness on flow over a circular cylinder and flapped aerofoil. *American Society of Mechanical Engineers, Fluids Engineering Division (Publication) FED 237*, 845-853.
- Cho SK, An HC, Shin JK, Yang YS and Park CD. 2005. Study on the development of trawl escapement device. *J Kor Soc Fish Technol* 41, 241-247.
- Chopin F and Suuronen P. 2009. The development of international guidelines on bycatch management and reduction of discards. *ICES CM 2009/M:01*.
- Diehl M, Magni L and Nicolao G. 2004. Efficient NMPC of unstable periodic systems using approximate infinite horizon closed loop costing. *Annual Rev Control* 28, 37-45.
- Ferro RST and Kynoch RJ. 2007. A square mesh panel in a Nephrops trawl, with an inclined guiding panel, to improve whitefish selection. *Fisheries Research*

- Services Collaborate Report No 02/07. Marine Laboratory, Aberdeen.
- Gavalda X, Ferrer-Gener J, Kopp GA, Giralt F and Galsworthy J. 2009. Simulating pressure coefficients on a circular cylinder at  $Re=10^6$  by cognitive classifiers. *Computers and Structures* 87, 838-846.
- Glass CW and Wardle CS. 1995. Studies on the use of visual stimuli to control fish escape from codend. II. The effect of a black tunnel on the reaction behaviour of fish in otter trawl codends. *Fish Res* 23, 165-174.
- Graham N, Jones EG and Reid DG. 2004. Review of technological advances for the study of fish behaviour in relation to demersal fishing trawls. *ICES J Mar Sci* 61, 1036-1043.
- Grimaldo E, Sistiaga M and Larsen RB. 2008. Evaluation of codends with sorting grids, exit windows, and diamond meshes: Size selection and fish behaviour. *Fish Res* 91, 271-280.
- Houska B, and Diehl M. 2006. Optimal control of towing kites. *Proc IEEE Conference on Decision and Control*, art. no. 4177402, 2693-2697.
- Jackson PS. 2005. Optimum loading of a tension kite. *AIAA Journal* 43(11), 2273-2278.
- Jones EG, Summerbell K and O'Neill FG. 2008. The influence of towing speed and fish density on the behaviour of haddock in a trawl cod-end. *Fish Res* 94, 166-174.
- Kim YH and Jang CY. 2005. Swimming characteristics of the black porgy *Acanthopagrus schlegeli* in the towing cod-end of a trawl. *J Fish Sci Technol* 8, 177-181.
- Kim YH and Wardle CS. 1998. Modelling the visual stimulus of towed fishing gear. *Fish Res* 34, 165-177.
- Kim YH and Wardle CS. 2003. Optomotor response and erratic response: quantitative analysis of fish reaction to towed fishing gears. *Fish Res* 60, 455-470.
- Kim YH and Wardle CS. 2006. Quantitative analysis of the swimming movements of flatfish reacting to the ground gear of bottom trawls. *J Fish Sci Technol* 9, 167-174.
- Kim YH, Wardle CS and An YS. 2008. Herding and escaping responses of juvenile roundfish to square mesh window in a trawl cod end. *Fish Sci* 74, 1-7.
- Macbeth WG, Broadhurst MK, Millar RB and Smith SDA. 2005. Increasing codend mesh openings: An appropriate strategy for improving the selectivity of penaeid fishing gears in an Australian estuary? *Mar & Fresh Res* 56, 889-900.
- Main J and Sangster GI. 1991. A study of haddock (*Merlanogrammus aeglefinus*(L.)) behaviour in diamond and square mesh cod-ends. *Scot Fish Work Paper* 19, pp.8.
- Massuti E, Ordines F and Guijarro B. 2009. Efficiency of flexible sorting grids to improve size selectivity of the bottom trawl in the Balearic Island (western Mediterranean), with comparison to a change in mesh cod-end geometry. *J Appl Ichthyol* 25, 153-161.
- Norberg C. 2003. Fluctuating lift on a circular cylinder: review and new measurements. *J Fluids and Structures* 17, 57-96.
- O'Neill FG, Kynoch RJ and Fryer RJ. 2006. Square mesh panels in North Sea demersal trawls: Separate estimates of panel and cod-end selectivity. *Fish Res* 78, 333-341.
- O'Neill FG, McKay SJ, Ward JN, Strickland A, Kynoch RJ and Zuur AF. 2003. An investigation of the relationship between sea state induced vessel motion and cod-end selection. *Fish Res* 60, 107-130.
- Polet H, Coenjaerts J and Verschoore R. 2004. Evaluation of the sieve nets as a selectivity-improving device in the Belgian brown shrimp (*Crangon crangon*) fishery. *Fish Res* 69, 35-48.
- Robertson JHB. 1986. Design and construction of square mesh cod-ends. *Scot Fish Infor. Pamphlet* 12, pp.10.
- Sala A, Lucchetti A, Piccinetti C and Ferretti M. 2008. Size selection by diamond- and square-mesh codends in multi-species Mediterranean demersal trawl fisheries. *Fish Res* 93, 8-21.
- Sánchez G. 2006. Dynamics and control of single-line kites. *Aeronautical J* 110, 615-622.
- Schlichting H. 1979. *Boundary-layer theory*. 7<sup>th</sup> Ed., Translated by Kestin J, McGraw-Hill book. Inc., New York, USA., 16-19, 657-664.
- Stevenson J, Alexander K and Lynn P. 2005. Kite performance testing by flying in a circle. *Aeronautical J* 109, 269-276.
- Vaikil A and Green SI. 2009. Drag and lift coefficients of inclined finite circular cylinders at moderate Reynolds numbers. *Computers Fluids* 38, 1771-1781.
- Wardle CS. 1993. Fish behaviour and fishing gear. In: *Behaviour of Teleost Fishes*. 2nd Ed., Pitcher T.J. ed. Chapman & Hall, London, UK., 609-644.
- Williams P, Lansdorp B and Ockels W. 2007. Flexible tethered kite with moveable attachment points, part I: Dynamics and control. *Collection of Technical Papers-2007 AIAA Atmospheric Flight Mechanics Conference* 2, 994-1017.
- Winkel H-J, Paschen M. 2005. Hydrodynamic loads on twisted ropes and hawsers. *Proceedings of the International Conference on Offshore Mechanics and Arctic Engineering - OMAE* 2, art. no. OMAE2005-67374, 775-777.

(Received 25 March 2010; Revised 26 May 2010;  
Accepted 10 June 2010)